

# Neural representation of $\alpha$ -oriented moving light bars in the cortex: A neural network study

Yihua Li<sup>1</sup> and Aike Guo<sup>1,2,\*</sup>

<sup>1</sup>Laboratory of Visual Information Processing, Institute of Biophysics, Chinese Academy of Sciences, Beijing 100101, People's Republic of China

<sup>2</sup>Institute of Neuroscience, Chinese Academy of Sciences, Shanghai 200031, People's Republic of China

(Received 12 July 1999 revised manuscript received 7 February 2001; published 26 September 2001)

A neural computational model is suggested in this paper for investigating the stimulus dependence of spiking patterns and the neural representation of  $\alpha$ -oriented moving light bars in the cortex. In this model, a stimulus-directed cortical developing algorithm is introduced for training the neural network. Three classes of computer simulations concerned with the orientation of the stimulus are carried out. The simulation results show that the fine temporal structure of spiking patterns of single units depends on the  $\alpha$  orientation of the two moving light bars, and the fine temporal structure of their combinatorial spiking patterns are also context dependent. They also show that the neural representation of an  $\alpha$ -oriented moving light bar is determined not only by the stimulus itself but also the architecture of the matured network. In the end, we propose a possible neural coding mechanism underlying the temporal cell subassemblies in the cortex, which could be spontaneously and dynamically organized into a dynamical cell assembly by synchronized activity of these subassemblies.

DOI: 10.1103/PhysRevE.64.041916

PACS number(s): 87.18.Sn, 87.19.La

## INTRODUCTION

How information can be integrated and how coherent representational states can be established in the cerebral cortex still attract much attention. For decades, most neurophysiologists have assumed that a neuron's information is contained solely in its mean firing rate. An alternative view, that temporal firing patterns contain information, is gaining attention as a result of recent theoretical and experimental approaches. Moreover, information coding in the cerebral cortex by independent or coordinated populations is also the subject of vigorous debate (see Ref. [1] for a review). The brain, however, most likely represents a world using neural assemblies, and population codes could be subtler. Over the years, a number of different definitions of "neural assembly" have been proposed. Some of them were defined in terms of anatomy, and others in terms of shared function or shared stimulus evoking responses (see Ref. [2] for review). Recently, a concept of dynamic cell assembly in the cortex was suggested by Fujii *et al.* [3]. However, whenever the population codes or assembly codes, a common problem that needs to be addressed is the binding problem. It was proposed that the synchronization of neuronal responses on a time scale of milliseconds might be a more efficient neural mechanism for binding the population response [4]. It was suggested cortical oscillations in the  $\gamma$ -frequency band (20–70 Hz) might be involved in an object representation [5], using the temporal structure to perform feature binding, but the hypothesis is still controversial (see Ref. [6] for a review). There is some evidence that the coherence of  $\gamma$ -band EEG activity could be as a basis for associative learning [7].

How to represent an essential feature of a perceptual object, and how to bind these features as an integrated whole in the cerebral cortex, still remain unresolved. In this paper we attempt to explore the representation mechanism of the two-moving-bar features, and to understand how the orientation of the stimulus and other features are bound into more complex features.

## MODEL

Our model is shown in Fig. 1. In Fig. 1(a), the upper is an input pattern, a state with two moving bars; the middle is the input layer of the network, and the bottom the cortical array. The input layer consists of two  $10 \times 10$  square arrays of input-layered units; the cortical array is a  $30 \times 30$  square array of cortical units. For the convenience of description, we number all 900 units by their locations (row, column),  $30 \times \text{row} + \text{column}$ . Figure 1(b) plots the response of input-layered units expressed by sombrero function.

A moving light bar is usually used as a visual stimulus in neurophysiological experiments for monkeys or cats awake or under anesthesia. In our simulations, two moving bars is accepted as the stimulus. They are of the same  $\alpha$  orientation, and move appositely at the same constant velocity  $v_0$  [Fig. 1(c)]. In all computer simulations, only the orientation  $\alpha$  for all parameters of the stimulus is considered. For the sake of discrete computation, it is digitized as a sequence of moving states of two moving bars. Each state is represented by  $10 \times 10$  array of blocks [also see Fig. 1(a)]. White blocks indicate the background, and all black blocks represent the two bars [see Fig. 1(c)]. In our simulations, each input pattern is applied to two square arrays of input layer at the same time (in Fig. 1). Each input-layered unit transforms the sum of inputs it receives, weighted by the sombrero function, into spikes and conveys them to the cortical array. The mathematics details for the transformation algorithm is given in Appendix A.

Our model is a modified copy of Shrager *et al.*'s version.

\*Author to whom correspondence and requests for materials should be addressed. Tel. 086-021-64853625; 086-010-64888533; Fax 086-010-64877837; email address: akguo@ion.ac.cn

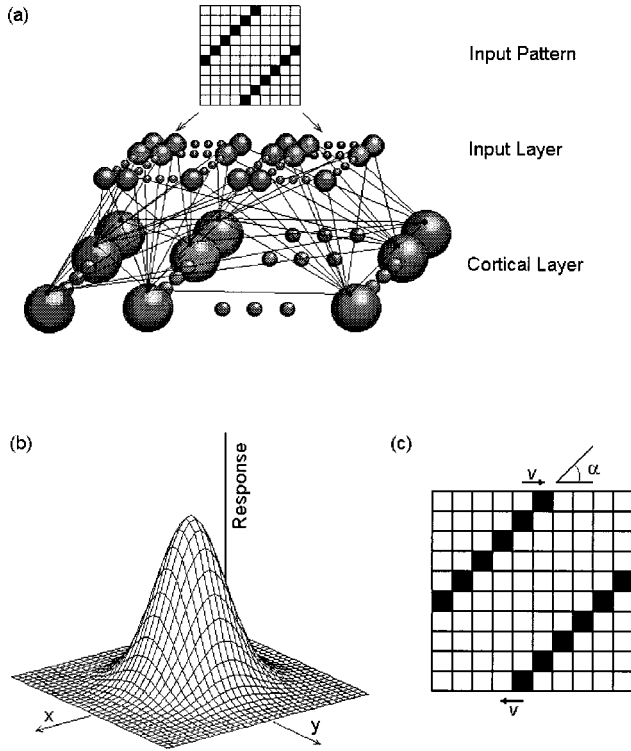


FIG. 1. Organization of the neural network model and the input pattern. (a) Diagram of the two-layered network, consisting of two square arrays of input-layered units and a square array of cortical units. (b) The response of the input-layered unit to the input pattern. (c) The stimulus:  $\alpha$ -oriented moving bars (the arrow indicates the moving direction of the bar).

Shrager *et al.* used a cortical array model based on the KDC model to investigate the emergence of a functional organization. According to the KDC model [8], the dendritic selection and elimination depend upon the activity-dependent diffusion of a neurotrophic substance (also see Ref. [9]). Shrager *et al.* [10] extended the KDC model by introducing a “wave” of plasticity, which can lead to a differential distribution of the function over the cortical surface, and revealed that this manipulation could induce the development of higher order functionality in subsequently developing areas of the simulated cortex.

In comparison with the version of Ref. [10], the most important modifications we made include the following: (1) Cortical units in the network are modeled by coincidence detector neurons. (2) The time delay to transmit a spike along a connection is considered, as well as the time delay to fire a spike by a neuron when its membrane potential is over its threshold. (3) The input layer consists of two square arrays of input-layered units, instead of input of two one-bit of afferent units [10]. (4) The cortical development algorithm (see Ref. [10]) is extended in accordance with the modifications of neuron model, time delay, and the firing property of input-layered units. (5) The associative learning rule is used in the training stage of the network, whereas in the subsequent testing stage for the matured network, the spike-based Hebbian learning rule [11] is employed.

All above modifications are based on the previous studies

and considerations. According to Softky [12], a cortical neuron functions as a coincidence detector at least in an effective sense. A coincidence detector neuron operates as a detector for the temporal coincidence of enough synaptic inputs to trigger the firing of the neuron [12,13]. Hopfield described an encoding and computation model using action potential timing to carry and encode information, and using a time-delay network to compute this representation. He suggested that the dynamic range and accuracy of the pattern recognition depend on the time resolution available [14]. Recently, studying distributed synaptic modification in neural networks induced by local stimulation with temporal patterns, Bi and Poo found that repetitive local stimulation can result in synaptic modifications at sites remote from the stimulated neuron [15]. Other documents indicated that time delay may be one of the origins of synchronized activity in the system (see Ref. [6] for a review). Time delay (or latency) is a potential code for feature binding in the striate cortex [16]. According to neurophysiological experiments, Watanabe and Aihara gave a mathematical expression that reflects the relationship between the strength of the superthreshold stimulation and the latency of action potentials [17]. These studies illustrated that time delay plays an important role in the neural coding, the neural representation, and the modification of synapses.

At the beginning of any simulation, as well as in the input layer, each unit in the cortical layer is randomly assigned to be excitatory or inhibitory. The probability of the excitatory cortical unit  $P_{\text{cell}}$  and the probability of the excitatory input-layered unit  $P_{\text{afferent}}$  are initially given. Whether the synaptic connections of a projective unit are excitatory or inhibitory, it is in accord with type of the unit. The inhibitory connectivity is local, while the excitatory connectivity is global. The projecting probability for an inhibitory presynaptic cortical unit  $j$  to post-synaptic unit  $i$  decays in an exponential way with distance,  $r = r(i, j)$ ,  $P_{\text{link}_i}(i, j) = A_i \exp(-r^2/2\pi\sigma_i)$ ; for the excitatory presynaptic cortical unit  $j$ , the projecting probability is  $P_{\text{link}_e}(i, j) = A_e$ . The synaptic connections from the input-layered unit to the cortical array are determined by the projecting probability  $P_{\text{link}_{ic}}$ , but there is no synaptic connection feedback to the input-layered units. To focus on the dynamics of the cortical array, the weight  $W_{kl}$  of the connection from input-layered unit  $k$  to the cortical neuron  $l$  is assigned to  $\varpi$  ( $\varpi = 0.8$  for all  $W_{kl}$ ). There is no synaptic connection from an input-layered unit to another input-layered unit or to itself, nor a synaptic connection from one cortical unit to itself in this model. Transmission spike delay along a synaptic connection is determined by the equation  $T_{\text{delay}} = B_k + C_k R(\cdot)$ , ( $k = cc, ic$ ), where  $R(\cdot)$  is a random function ranging from 0.0 to 1.0.  $B_k$  and  $C_k$  are constants.  $cc$  indicates the synaptic connection of one cortical unit to another cortical unit, and  $ic$  from that of an input-layered unit to a cortical unit. Once the distribution of intercortical connections is assigned, the initial threshold  $\Theta_v$  of cortical unit  $v$  and the initial weight  $W_{uv}$  of the intercortical connection (cortical unit  $u$  to unit  $v$ ) are thus determined (see Appendix A).

With the initialized network, the training operation of the network and the testing are carried out in turn. For the training operation, a brief summary of the mathematical details

TABLE I. The values of most important simulation parameters of the model.  $\chi_{ij}$  is the concentration of trophic factor (initially  $\chi_{ij}=0$  for all connections), and the other parameters in the developing process are the same as in Ref. [10].

Variable	Parameter	Value
$P_{\text{cell}}$	the ratio of cortical excitatory units to the inhibitory synapse connection	0.5–0.8
$P_{\text{afferent}}$	the ratio of input-layered excitatory units to the inhibitory synapse connections	0.3–0.8
$A_i, \sigma_i$	the coefficients for initially assigning the cortical inhibitory synapse connections	0.6, 5
$A_e$	the coefficients for initially assigning the cortical excitatory synapse connections	0.1–0.45
$P_{\text{link } ic}$	the probability for initially assigning the synapse connections from input-layered units to a cortical array	0.25
$B_{cc}, C_{cc}$	intercortical transmission delay constant	1 cycle (ms), 20 cycles (ms)
$B_{ic}, C_{ic}$	input-layered units to the cortical units transmission delay constant	8 cycles (ms), 4 cycles (ms)
$T_0, T_+$	threshold constant of cortical units	7.0, 0.25
$T_i$	threshold of cortical unit $i$	$T_i = T_0 + T_+ \sum W_{ij}$
$a_0, b_0$	cortical synapse weight constant	1, 0.4
$W_{ij}$	synaptic strength	$W_{ij} = a_0 + b_0^* \chi_{ij}$
$T_{\text{sleep}}$	absolute refractory period	5–7 cycles (ms)
$\eta$	learning parameter	$1.0e-5$
$\tau^{\text{syn}}$	time constant	5 cycles (ms)
$\tau_+$	time constant	1 cycle (ms)
$\tau_-$	time constant	20 cycles (ms)
$A_+$	dimensionless constant	1.0
$A_-$	dimensionless constant	-1.0

for the development algorithm is given in Appendix A, and a subset of the most important model's parameters are shown in Table I. These parameters were assigned to single units, synapses, or channels. More details of the cortical development algorithm can be found in Refs. [10] and [8]. As a result of the training operation, one striking aspect of the development of the cortical array in the network is stimulus-directed pruning of the initial overproduction of synaptic connections, resulting in a relatively sparsely interconnected final functional architecture. In addition, the parameters for the matured network, such as threshold  $\Theta_v$  of neuron  $v$ , the weight  $W_{u,v}$  of connection (from  $u$  to  $v$ ), the transmission delay  $TD_{u,v}$  of the connection (synaptic pathway), and the spatial distribution of the remaining intercortical connections, are closely correlated to the given training stimulus. In subsequent testing process, instead of Hebb's association

rule used in the training process, a spike-based Hebbian learning rule depending critically on an asymmetric "learning window" [11] was adopted. The change of the synaptic weight  $\Delta W_{ij}$  depends only on firing times  $t_i^f$  (the arrival time of the  $f$ th input spike at neuron  $i$ ) and  $t^n$  (the  $n$ th output spike of the neuron) in the time interval  $[t, t + \Delta T]$ ,

$$\Delta W_{ij} = \eta \left[ \sum_{t_i^f} 'w^{\text{in}} + \sum_{t^n} 'w^{\text{out}} + \sum_{t_i^f, t^n} 'W(t_i^f - t^n) \right],$$

where the learning parameters  $w^{\text{in}}$  and  $w^{\text{in}}$  are related to  $\eta$ ,  $w^{\text{in}} = \eta$  and  $w^{\text{in}} = -1.0475 \eta$ . The learning window  $W(s)$  in units of the learning parameter  $\eta$  is a function of the delay  $s = t_i^f - t^n$ ,

$$W(s) = \eta \begin{cases} \exp\left(\frac{S}{\tau^{\text{syn}}}\right) \left[ A_+ \left(1 - \frac{S}{\tau_+}\right) + A_- \left(1 - \frac{S}{\tau_-}\right) \right] & \text{for } S \leq 0 \\ A_+ \exp\left(-\frac{S}{\tau_+}\right) + A_- \exp\left(-\frac{S}{\tau_-}\right) & \text{for } S > 0, \end{cases}$$

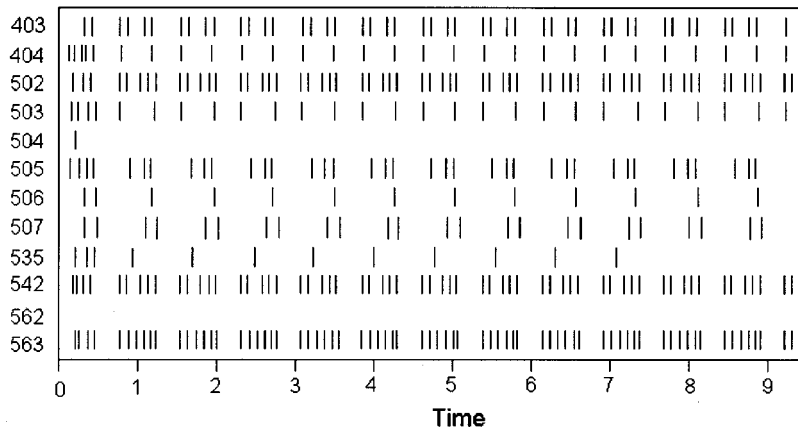


FIG. 2. The spike trains of 12 out of 900 cortical units on the testing stimulus, a  $30^\circ$ -oriented moving bars, for the network trained by the training stimulus, a  $30^\circ$ -oriented moving bar, with the stimulus parameters  $v_0=1$  and stimulation conditions listed in Table I.

where  $\tau^{\text{syn}}$ ,  $\tau_+$ ,  $\tau_-$ ,  $\tilde{\tau}_+ = \tau^{\text{syn}}\tau_+ / (\tau^{\text{syn}} + \tau_+)$  and  $\tilde{\tau}_- = \tau^{\text{syn}}\tau_- / (\tau^{\text{syn}} + \tau_-)$  are time constants. In the testing operation the modification of the transmission spike delays the synaptic connections and the changes of thresholds for cortical units, as well as a pruning of the synaptic connections, were considered less than in training process.

### SIMULATION RESULTS

As described above, all simulations we made include two steps: a training network and a subsequent testing operation. The stimulus used in a specific stage is thus called the training stimulus or testing stimulus. For the convenience of description, we let  $\beta$  denote the orientation of the training stimulus for the training stage, and  $\alpha$  the orientation of the testing stimulus for the testing stage. In order to investigate the neural representation of  $\alpha$ -orientated two moving bars, three classes of simulations are designed in this study. We now describe them in detail.

In the first class of simulations, the same stimulus serves to train the network and then to test it. An example described here is the case of the chief stimulus parameters  $v_0=1$  (blocks per training phase),  $\alpha=\beta=30^\circ$ . Typical results of the training operation include the fact that the synaptic connection density become relatively sparse. Synaptic connections within the cortical array are reduced by 71.8%. Before the training operation, a cortical unit receives an average of 47.6 connections from other cortical units, but there are only 13.4 connections remaining on average after the training processing. In addition, the transmission spike delay and weight for every intercortical connection are modified, and the threshold for every cortical unit is adjusted. Figure 2 plots the 12 spike trains of 12 cortical units firings with 12 repetitive inputs of the same stimulus in the testing stage. Before analyzing the temporal structure of spiking timings of single units, we simply define the spiking pattern of a single unit as repetition pattern in its spike train. In Fig. 2, it can clearly be seen that in every spike train, all but the first several spikes in each activated unit precisely respond to the given input in a specific spiking pattern. The time interval between alternate repetition patterns in the spike train depends on the interval of the input stimulus,  $T_{\text{int}}$ . It is very interesting that in the auditory cortex of mammals, the spiking patterns of

single cell responses to specific calls are reproduced from trial to trial with millisecond precision [18,19].

In the second class of simulations, one network is first trained on the condition of two moving bars that are  $\beta$ -oriented. Then a variety of  $\alpha_1, \alpha_2, \dots, \alpha_k$ -orientated two-moving-bar testing stimuli are separately applied to the matured network for testing. The simulation examples reported here are carried out with the chief stimulus parameters  $\beta=30^\circ$  for training, and  $\alpha_1=30^\circ$ ,  $\alpha_2=45^\circ$ ,  $\alpha_3=0^\circ$ , and  $\alpha_4=90^\circ$  for testing. For the convenience of description, these testing simulations are separately defined as Example A ( $\alpha_1=30^\circ$ ), Example B ( $\alpha_2=45^\circ$ ), Example C ( $\alpha_3=0^\circ$ ) and Example D ( $\alpha_4=90^\circ$ ). With the given four simulation experiments, 80 out of 900 cortical units, 324th–403th, marked as 0–79, are selected for analyzing the responses of cortical units. In Figs. 3(a), 3(b), 3(c), and 3(d), most of the spike trains indicate that although the given stimulus is different, most of single units fire in specific spiking patterns, and the time interval between alternate repetition pattern in every spike train is associated with the interval of the repetitive input. Even so, for these units, the spiking patterns of the same unit in different experiments are not the same. In the simulation experiment, Example A, as illustrated above, when the testing stimulus is the same as the training stimulus ( $\alpha=\beta$ ), all activated units precisely repeatedly respond to the given input in the manner of specific spiking patterns. However, when the testing stimulus is different from the training stimulus ( $\alpha\neq\beta$ ) with regard to the firing pattern and its temporal structure, some changes appears. For instance, in Example B, the testing stimulus parameter is  $\beta=30^\circ$ , and the training stimulus parameter  $\alpha=45^\circ$ . As displayed in Fig. 4, for every spike train, during the first few repetition inputs, the spiking patterns of some single units change from one temporal structure to another (e.g., units 141 and 234 in Fig. 4). Some units begin to stop firing (i.e., unit 402) or begin to fire (i.e., unit 660). Their firings transit from a temporal structure (or spike pattern) to another structure. This result reveals that if the orientation of the testing stimulus is different from that of the training stimulus stored in the network, the nonlinear dynamic evolution of the system will appear. It will finish in a short time and run in a stable state. The nonlinear dynamic evolution process of the system further illustrates the dynamic behavior robustness of the network

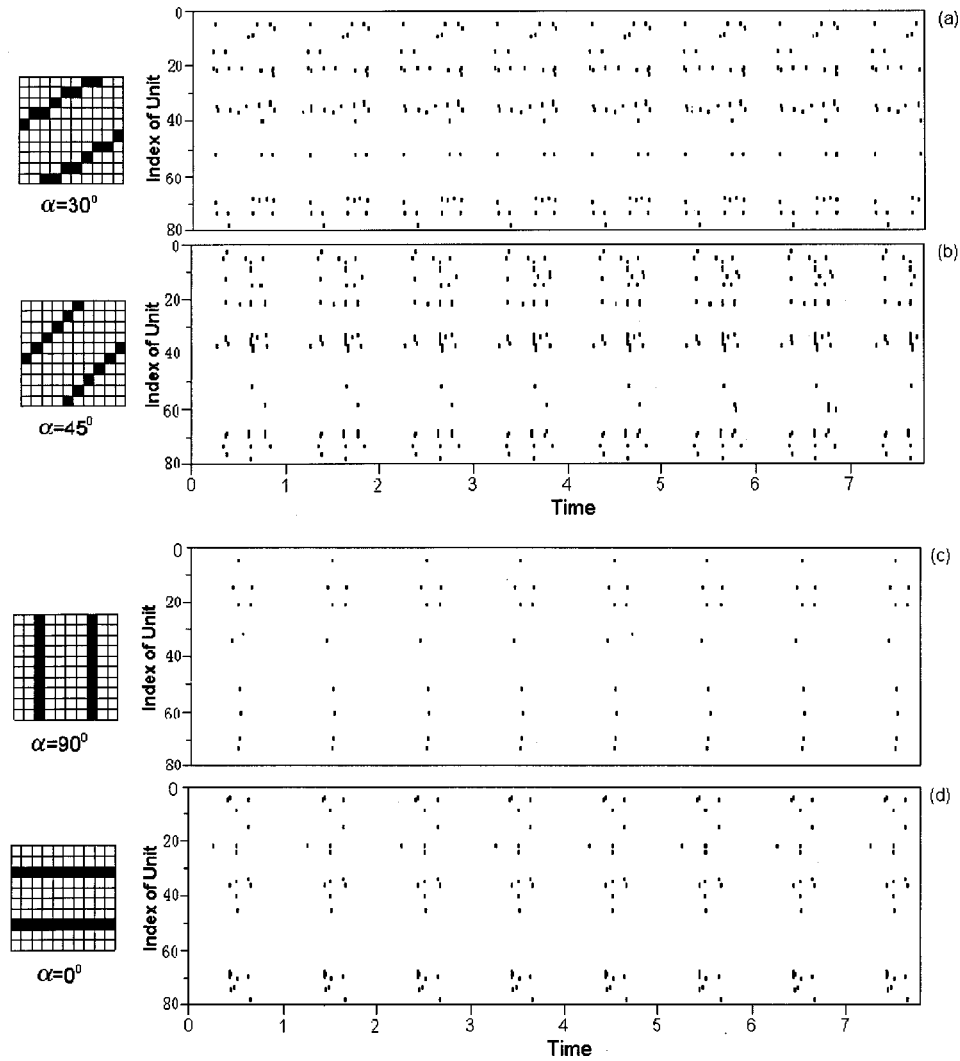


FIG. 3. The spike trains of 80 out of 900 cortical units (located at 0–79 in the cortical array) on the specific stimulus,  $\alpha$ -oriented moving bars ( $\alpha=0^\circ$ ,  $\alpha=30^\circ$ ,  $\alpha=45^\circ$ , and  $\alpha=90^\circ$ , respectively), with the other simulation parameters and simulation conditions as in Fig. 2.

model. When firing single units from one spiking pattern to another spiking pattern, the temporal structure of their combinatorial spiking patterns change to a new temporal structure. Thus, in the sense of neural representation of an  $\alpha$ -orientated two moving bar, information may be encoded in combinatorial spiking patterns more than in the firing patterns of single units.

For a given simulation experiment, in the light of the fine temporal structure of the spiking patterns, all cortical units firings could be categorized. For two units  $u$  and  $v$ , if the temporal structures of their spiking patterns are the same, their firings could be categorized as the same  $a$  class. Otherwise, their firings are categorized in two different classes. Statistical data show that for the four simulation experiments, the counts for the classes of spiking patterns are 70

for Example A ( $\alpha_2=30^\circ$ ), 77 for Example B ( $\alpha_3=45^\circ$ ), 23 for Example C ( $\alpha_1=0^\circ$ ), and 28 for Example D ( $\alpha_4=90^\circ$ ), respectively. It seems that in a neural representation of  $\alpha$ -oriented two moving bars, if only comparing the counts for the classes of spiking patterns to represent the stimulus, two moving bars that are oriented  $30^\circ$  or  $45^\circ$ , is more than the cases of  $0^\circ$ - or  $90^\circ$ -orientated two moving bars. On the other hand, we note that although the orientations of the testing stimuli are different, the same spiking patterns always exist among the four different simulation experiments. The phenomena also appear in the case of nonlinear dynamic evolution of single units discharges. When the system is running in a stable state, the spiking patterns of single units firings (not generated by the same unit) can be also found in the neural representations of the other stimuli. The result

TABLE II. The maximum crosscorrelation coefficient  $\rho_{\max}$  between two frequencies of firing frames of the cortical array on the same testing stimulus, a  $30^\circ$ -oriented bars, for the two different networks trained separately by two moving bars oriented by  $\beta_1$  and  $\beta_2$  (Ave. indicates average and Vari. variance)

$\beta_1, \beta_2$	$0^\circ, 30^\circ$	$0^\circ, 60^\circ$	$0^\circ, 120^\circ$	$30^\circ, 60^\circ$	$30^\circ, 120^\circ$	$60^\circ, 120^\circ$	Ave.	Vari.
$\rho_{\max}$	0.03	0.08	0.08	0.07	0.02	0.07	0.06	$2.8 \times 10^{-3}$

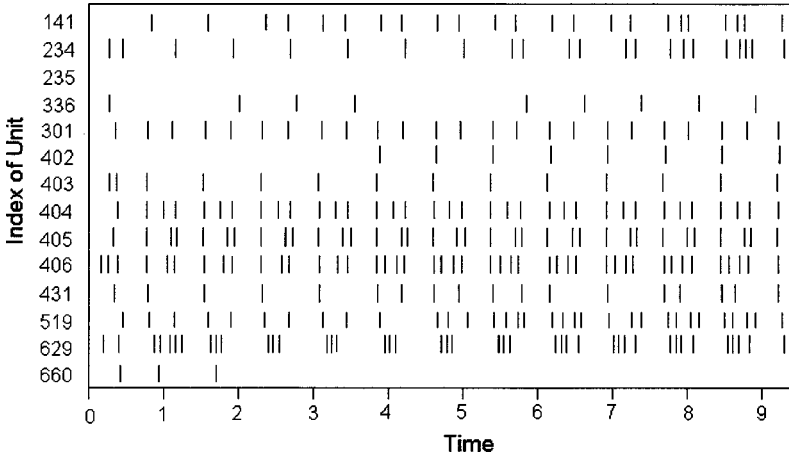


FIG. 4. The spike trains of 14 units on the testing stimulus, a  $45^\circ$ -oriented moving bars, for the network trained by the training stimulus, a  $30^\circ$ -oriented moving bars, with the same stimulus parameters and simulation conditions as in Fig. 2.

illuminates that the responses of cortical units are selectively involved in representation of stimulus in manner of spiking patterns. Thus, the exacting timing of individual spikes is correlated to a specific stimulus, and the combination of spiking patterns of individual units is context-dependent.

Carefully analyzing the firings of the individual units, we find that the activity of the activated units within the cortical array includes both arrhythmic spiking and rhythmic spiking. An oscillatory analysis of the units firings by identification of power spectrum peaks indicates that with a given stimulus, a two moving bar oriented by  $30^\circ$ , oscillatory firings of single units exist in the frequency range 13–72 Hz. The same data can be obtained in the other simulation experiments (Examples B, C, and D). The data of the frequency range for these single units seem to not be correlated to the orientation of the stimulus. These data are in agreement with the previous experimental data [20–23]. We also note that some units are still suppressed, i.e., units 504 and 562 (in Fig. 2).

In order to describe the collective responses of the cortical array and further examine the response properties of units in this representation, we turn to an analysis of the responses of the whole cortical array. During a simulation operation, the instantaneous firing states of all units within a cortical array at a time  $t_i$  form a binary image if the active state of a unit is denoted by the pixel value 1, and an inactive state by 0. Here every binary image could be called a firing frame for describing the instantaneous firing states of the cortical array. Because one firing frame is formed at each running step, a sequence of firing frames is yielded during the testing process. According to our definition of autocorrelation for the activity of the cortical array (see Appendix B), we examine the power spectrum of combinatorial spiking patterns of the cortical array in Example A. The data demonstrate that the

synchronization of the oscillating activity of the cortical array occurs in frequencies  $14 \pm 2$  and  $44 \pm 3$  Hz. The first peak in the power spectrum is in the  $\alpha$ -frequency band, and the other is in the  $\gamma$ -frequency band. Some papers suggested that the coherence of the fast rhythms emerges within a short range, whereas low-frequency sleep rhythms exhibit synchronization on a larger spatial scale [24–26]. If it is true that the cortical array developing process can cause a differential distribution of functions over the cortical array suggested in Ref. [10], the low-frequency peak ( $14 \pm 2$  Hz) may reveal a synchronization of cells among two or more separated function structures. Therefore, for the experiment (Example A), there is more than one synchronous episode of groups of units in neural representation of two moving bars oriented  $30^\circ$ . Similar calculations for the other three experiments were carried out, and the same conclusion achieved.

For the third class of simulations, a variety of  $\beta$ -oriented bars,  $\beta_1 = 0^\circ$ ,  $\beta_2 = 30^\circ$ ,  $\beta_3 = 45^\circ$ ,  $\beta_4 = 90^\circ$ , are separately used for training four different networks. Then the same stimulus, a  $30^\circ$ -oriented bar, is applied to these mature networks for the testing operation. In order to evaluate collective response properties of the cortical array, we introduce a cross-correlation analysis for the responses of the cortical array (see Appendix B). Table II lists the maximum cross-correlation coefficients between the two sequences of firing frames of the cortical array in the condition of the same testing stimulus ( $\alpha = 30^\circ$ ) for two different networks trained separately by two different training stimuli,  $\beta_1$ - and  $\beta_2$ -oriented bars. In comparison with this result, Table III lists the maximum cross-correlation coefficients between the two sequences of firing frames of the cortical array under conditions of two different testing stimuli,  $\alpha_1$ - and  $\alpha_2$ -oriented bars, for the same network trained by a  $30^\circ$ -oriented bar. It can be seen that the coefficients in Table III

TABLE III. The maximum crosscorrelation coefficient  $\rho_{\max}$  between the two frequencies of the cortical array on the two different stimuli, two moving bars oriented by  $\alpha_1$  and  $\alpha_2$ , for the same network trained by training stimulus, a  $30^\circ$ -oriented bar ( $\beta = 30^\circ$ ).

$\alpha_1, \alpha_2$	$0^\circ, 30^\circ$	$0^\circ, 45^\circ$	$0^\circ, 90^\circ$	$30^\circ, 30^\circ$	$30^\circ, 45^\circ$	$30^\circ, 90^\circ$	$45^\circ, 90^\circ$	Ave.	Vari.
$\rho_{\max}$	0.16	0.24	0.29	1.00	0.24	0.21	0.19	0.63	1.21

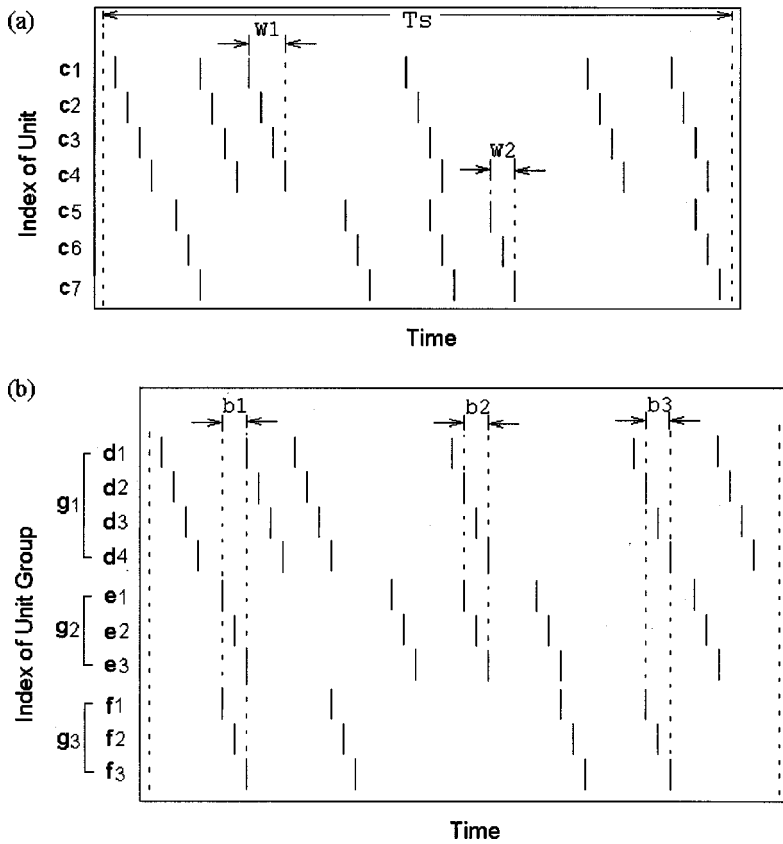


FIG. 5. (a) The scheme of a temporal cell assembly and its two temporal cell subassemblies. Each short line indicates a spike.  $w_1$  and  $w_2$  denote respective activity bins of temporal cell subassemblies ( $c_1$ – $c_4$  and  $c_5$ – $c_7$ ). (b) Demonstration of the episode of synchrony and desynchrony among temporal cell subassemblies ( $g_1$ – $g_3$ ).  $b_1$ – $b_3$  denote relative precise and timing overlapping windows between temporal cell subassemblies, in which synchronization of the components among temporal cell subassemblies results in the emergence of dynamic cell assemblies.

are much higher than the values in Table II. This result reveals that the responses of the two different networks trained by different stimuli in neural representations of the same stimulus are obviously different. This is accordance with the conclusion that the network pathway remodeling inducing by repetitive local stimulation appears to be highly dependent on a precise temporal pattern of the stimulation [15]. The combination of spiking patterns of all cortical units within the cortical array depends not only on the stimulus itself but also on the final functional architecture of the mature network. These combinatorial spiking patterns may play a more important role in the neural representation of an  $\alpha$ -oriented bar than spiking timings for single cortical units. Abeles and co-workers reported that they detected repetition patterns in spike trains taken from multiple cell recordings [27–30]. They suggested that the spatiotemporal firing patterns related to behavior and information may be encoded in spatiotemporal firing patterns [28,29].

It is interesting in Table II that there are pairs with the same values: 0.07 for  $30^\circ$ – $60^\circ$  and  $90^\circ$ – $120^\circ$  and 0.08 for  $0^\circ$ – $60^\circ$  and  $0^\circ$ – $120^\circ$ . We find that for every pair of training stimuli with the same value, the differences in orientations of the two stimuli for its two items are the same. For example, the pairs  $30^\circ$ – $60^\circ$  and  $90^\circ$ – $120^\circ$  have the same coefficient 0.07, the differences between the two items are both  $30^\circ$ . The reason for this is that the response function of the input-layered units is the sombrero function with a circular received field.

## DISCUSSION AND CONCLUSION

### A possible spatiotemporal coding mechanism

Observing spiking patterns of some cortical units shows that there are cortical units responding to stimuli from the same fine temporal structure (e.g., units 502 and 542 in Fig. 2). These units could be thus defined as temporal cell assemblies. The response properties of the ensemble of units are similar to that of a functional column in the visual cortex, but these units could be spatially separated. Furthermore, if the phase relationship of spiking timings for every cortical unit in a temporal cell assembly is considered, a temporal cell assembly can be split into several temporal cell subassemblies, in which the activity of all components can form a closely firing chain [e.g., a subassembly in Fig. 5(a)]. In other words a temporal cell subassembly holds a time bin of activity, termed as the activity bin (i.e.,  $w_1$ ), in which all components fire in turn. Motivated by the characteristics of a functional column and a functional microcolumn, we postulate that a temporal cell subassembly acts as a detector of local features.

The results of recent studies of the visual system indicated that responses to synchronously presented pattern elements can be bound together and interpreted as a part of the same object, whereas responses to pattern elements presented with temporal offsets more greater than 10 ms are perceived to be unrelated [31–33]. One can interpret synchrony as a signature of relatedness. Abeles and co-workers studied whether

repetition patterns in spike trains taken from multiple cell recordings are associated with an external event. They suggested that synfire reverberations offer some advantages with regard to the possibility of processes in different brain locations. The selective connections between cell assemblies are marked by temporal coherence on a millisecond time scale [4,34,35]. Together with the function of synchronization and our simulation results, we attempt to demonstrate a possible neural coding mechanism concerned with temporal cell subassemblies. Three temporal cell subassemblies [g1–g3, in Fig. 5(b)] are taken into account for the sake of simple interpretation. Within a large temporal window  $T_s$  [shown in Fig. 5(b)], if the overlap occurs among their activity bins (b1, b2, and b3, respectively), these temporal cell subassemblies (i.e., g1 and g2, g1 and g3) will fire synchronously within their overlap activity bin. Because the emergence of temporal cell assemblies results from an input event of coincidence detection by the mature network, these cell subassemblies thus establish a temporal correlative relationship underlying their characteristic spiking patterns. In these subassemblies, the cells firing within the overlap activity bin are functionally linked, temporally and they organized spontaneously into a dynamical cell assembly. Because of synchronization, the feature information contained in these temporal cell subassemblies is temporally bound together and conveyed to subsequent processing systems in a precise timing and consistent manner. The activity of the dynamical cell assembly, specific spatiotemporal firing patterns, carries more complex features. Thus the participation of all components in a temporal cell subassembly temporally contributes collectively to a particular coding function. This possible coding mechanism is in agreement with an electrophysiological experiment. The detailed structure of the columnar organization was investigated by using optical imaging of the intrinsic signal. The result suggests that there exists a grouping of columns representing related features, and that they cluster with partial overlaps to compose a large unit of image processing [36]. It was reported more recently that precisely reproducing temporal firing patterns in thalamocortical responses produces information about stimulus features [37,38]. Clearly, the selective feature’s binding mechanism depends on temporal aspects—the overlap among active bins, and the large temporal window nesting these small bins as well. Evidently, selective connections between cell assemblies are marked by temporal coherence on a millisecond time scale [4,39,40]. The coding strategy also indicates that if only a single feature is present or if overlap among the activity bins never occurs, then the binding problem does not arise. In fact, some project neuron pairs in insect olfactory system, whose components are both activated by the same odor, may never even fire spikes together synchronously [41].

Abeles and co-workers found that spatiotemporal firing patterns in the frontal areas of monkeys are associated with behavior. They suggested that information may be encoded in the spatiotemporal firing patterns as in the “synfire” model [28,29,42]. Watanabe, Aihara, and Kondo’s simulation experiments obtained the same conclusion on a spatiotemporal firing pattern [43]. However, the difference between con-

cerns whether the spiking patterns in the networks are synchronous or not. The synfire model assumes that firings of neurons in the same node are synchronized, while the latter assumes that dynamical cell assemblies could be organized in a network by a coincidence of incident pulses and a temporal correlation of firings resulting from events of such coincidence detection [3]. Our model is in agreement with that of Ref. [43]. We emphasize that the organization of dynamical cell assemblies results from a synchronization of firings among temporal cell subassemblies. We suggest that the emergence of temporal cell subassemblies is stimulus driven, and results from events of coincidence detection by the mature network. In our suggested coding mechanism, the overlap activity bin among temporal cell subassemblies provides a temporal window for synchronization of these subassemblies. Within the overlap activity bin, the neurons belonging to these temporal cell subassemblies are temporally linked and organized spontaneously into a dynamical cell assembly. A selective feature binding mechanism relies on the relative spiking timing among temporal cell assemblies and precise temporal windows. Synchronization among temporal cell subassemblies could be used for response selection and to organize a more complex cell assembly, because it enhances the saliency of discharges with great temporal selectivity, in accordance with the previous conclusion [44]. Thus, information may be encoded in the precise temporal relations among members of a dynamical cell assembly, and be encoded by spatiotemporal firing patterns.

In this research, three aspects of simulation experiments are carried out. The results demonstrate that responses of cortical units are selectively involved in a neural representation of stimulus in the manner of spiking patterns. The combination of spiking patterns of all cortical units depends not only on the stimulus itself but also on the final functional architecture of the network. It has been suggested that if spike timing encodes neural information, a delay line architecture combined with a spike timing-based synaptic modification rules provides a network mechanism, to convert and store temporal information into spatially distributed patterns of permanent synaptic modifications [15].

#### ACKNOWLEDGMENT

This research was funded by the NSFC (C01050103 and 69835020).

#### APPENDIX A: A CORTICAL DEVELOPMENT ALGORITHM

This appendix is adapted in part from Refs. [8] and [10]. At the beginning of the training procedure, each cortical unit has a firing threshold  $T_i$  and a pool of “trophic factor” ( $F_T$ ),  $\mu_i$  ( $\mu_i = 20.0$  for all units),

$$T_i(t) = T_0 + T_+ \sum_{W_{ij} > 0} W_{ij}, \quad (\text{A1})$$

where  $T_0 = 7.0$ , and  $T_+ = 0.2$ . The synaptic weight  $W_{ij}$  is related to the amount of  $F_T$  that accumulated in the connection, expressed as

$$W_{ij}(t) = c_0 + c_1 \sigma_{ij}, \quad (\text{A2})$$

where  $c_0 = 1.0$  and  $c_1 = 4.0$ .  $\sigma_{ij}$  is the concentration of  $F_T$  in the connection from unit  $i$  to unit  $j$ . Each connection between units take on one of three discrete states: labile, stable or dead. Initially, all connections begin in the labile state, and  $\sigma_{ij} = 0$ . A synaptic connection is essentially guaranteed to stabilize when its  $\sigma_{ij}$  reaches 1.0. Similarly, the probability of a connection entering the dead state is proportional to the time  $t$ , whose simulation runs

$$P_{\text{stabilize}} = 1/\{1 + \exp[-15(\sigma_{ij} - 1)]\}, \quad (\text{A3})$$

$$P_{\text{die}} = 1/\{1 + \exp[-0.02(t - 500)]\}. \quad (\text{A4})$$

In a simulation, the response function of a cortical unit is modeled by the response function of a cortical cell by a rectangular response function in an effective sense [45]. At each running cycle, within a quasisynchronous window  $\varpi$  ( $\varpi = 1.5$  cycles), each cortical unit sums the activation coming to it along excitatory connections and subtracts from inhibitory connections, both weighted by synaptic efficiencies  $W_{ij}$ . If the summation of the activation  $\mathcal{U}$  is over than its firing threshold  $T_i$ , and if no action potentials has been generated more recently the refractory period  $T_{\text{sleep}}$  ( $T_{\text{sleep}} = 4-7$  ms), it will emit a spike precisely behind the time delay  $\Delta t$ . The time delay is described by the function  $g(\mathcal{U}) = \theta/[\varphi + (\mathcal{U} - T_i)]$ , ( $\theta = 3-6$  ms and  $\varphi = 1.0$ ), which models a relationship between the strength of the superthreshold stimulation and the latency of the action potentials [17]. The transmission spike delay of each connection (synapse pathway) is modified by the covariance rule of the activity of presynaptic and post-synaptic neurons, according to the equation

$$\Delta T_d = -\rho(V_B - \langle V_B \rangle)(V_A - \langle V_A \rangle), \rho = 1.0 \times 10^{-5}.$$

At each training phase (every five cycles), the network is trained by updated  $\mu_i$ ,  $\sigma_{ij}$ , and  $T_i$  connection states. A quantity of  $F_T$  is moved from a unit pool of  $F_T(\mu_i)$  to a link pool of  $F_T(\sigma_{ij})$  according to a Hebbian associative rule. (1) For excitatory post-synaptic units,  $\delta_{\text{Hebb}} = 1$  whenever the pre-synaptic post-synaptic neurons fire simultaneously, and  $\delta_{\text{Hebb}} = 0$  otherwise. (2) For inhibitory terminals,  $\delta_{\text{Hebb}} = 1$  whenever the post-synaptic neuron fires but the presynaptic (inhibitory) neuron does not fire; otherwise,  $\delta_{\text{Hebb}} = 0$ . The concentration of  $F_T$  in an incoming connection  $\sigma_{ij}$  changes according to the following equations:

$$\Delta \mu_i = -0.01 \delta_{\text{Hebb}} \mu_i, \quad (\text{A5})$$

$$\Delta \sigma_{ij} = -\lambda_c(1) \Delta \mu_i. \quad (\text{A6})$$

Here the scaling factor  $\lambda_c(t)$  reflects a dynamic Gaussian spatial modulation of the diffusion across the cortical array. During the first training phase, the following value of  $\lambda_c$  will be utilized:

$$\lambda_c = \{1.0, 0.86, 0.77, 0.66, 0.53, \dots, 0.0\}.$$

On the next training phase, the ‘‘wave’’ of plasticity moves to the right a small amount.

$$\lambda_c = \{0.86, 1.0, 0.86, 0.77, 0.66, 0.53, \dots, 0.0\}.$$

The ‘‘wave’’ moves the same small amount for each training phase, with the end of the development manipulation. The firing threshold  $T_i$  of a cortical unit, or synaptic weight  $W_{ij}$ , and a connection state are updated according to the Eqs. (A1)–(A4).

Meanwhile, at each training phase, two square arrays of input layer simultaneously transform a stimulus pattern into bundles of spike trains with the specific spatiotemporal structure. The responses of an input-layered unit is determined by a pixel and its eight neighbors within input pattern.

$$\begin{aligned} y(i, j) = & a_0 x(i, j) + a_1 [x(i-1, j-1) + x(i+1, j-1) \\ & + x(i-1, j+1) + x(i+1, j+1)] \\ & + a_2 [x(i, j-1) + x(i, j+1) + x(i-1, j) \\ & + x(i+1, j)], \end{aligned} \quad (\text{A7})$$

where  $a_0 = 1.0$ ,  $a_1 = 0.77$ , and  $a_2 = 0.66$ . If  $y(i, j) > T_f$  ( $T_f = 1.0$ ), the input-layered unit emits a spike precise behind the time  $T_d = 6/[1.0 - (y(i, j) - T_f)]$ .

## APPENDIX B

With the two sequences of the firing frames of the cortical array in neural representations of the stimulus, we define the autocorrelation coefficient  $\rho_a(t_0)$  and the crosscorrelation coefficient  $\rho_c(t_0)$  as

$$\begin{aligned} \rho_a(t_0) &= \frac{1}{N} \sum_{t=1}^N \sum_{x,y=1}^D \delta[U(x, y, t+t_0) - U(x, y, t)], \\ \rho_c(t_0) &= \frac{1}{N} \sum_{t=1}^N \sum_{x,y=1}^D \delta[U_a(x, y, t+t_0) - U_b(x, y, t)], \end{aligned}$$

respectively, where  $\delta(\cdot)$  is the delta function, and  $N$  indicates the duration for computation,  $D$  its dimension, and  $U_a(x, y, t)$  and  $U_b(x, y, t)$  the activity of the neuron  $(x, y)$  responding to  $a$  and  $b$  stimuli at time  $t$ . Generally,  $N$  is set to the time interval between two repetitive inputs of the stimulus.

- [1] R. Christopher deCharms, Proc. Natl. Acad. Sci. U.S.A. **95**, 15 166 (1998).  
 [2] G. L. Gerstein, P. Bendenbaugh, and A. M. H. J. Aertsen, IEEE Trans. Biomed. Eng. **36**, 4 (1989).

- [3] H. Fujii, H. Ito, K. Aihara, N. Ichinose, and M. Tsukada, Neural Networks **9**, 1303 (1996).  
 [4] C. von der Malsburg, Ber. Bunsenges. Phys. Chem. **89**, 703 (1985).

- [5] W. Singer, in *The Handbook of Brain Theory and Neural Networks*, edited by M. A. Arabib (MIT Press, Cambridge, MA, 1995), pp. 960–964.
- [6] R. Ritz and T. J. Sejnowski, *Curr. Opin. Neurobiol.* **7**, 536 (1997).
- [7] H. R. Wolfgang, Christoph Brau Miltner, Matthias Arnod, Herbert Witte, and Edward Taub, *Nature (London)* **397**, 4 (1999).
- [8] M. Kerszberg, S. Dehaene, and J. P. Changeux, *Neural Networks* **5**, 403 (1992).
- [9] P. R. Montague, J. A. Gally, and G. M. Edelman, *Cerebral Cortex* **1**, 199 (1991).
- [10] J. Shrager and M. H. Johnson, *Neural Networks* **9**, 1119 (1996).
- [11] R. Kempster, W. Gerstner, and J. Leo van Hemmen, *Phys. Rev. E* **59**, 4498 (1999).
- [12] W. R. Softky, *Curr. Opin. Neurobiol.* **5**, 239 (1995).
- [13] M. Abeles, *Isr. J. Med. Sci.* **18**, 83 (1982).
- [14] J. J. Hopfield, *Nature (London)* **376**, 33 (1995).
- [15] G. Bi and M. Poo, *Nature (London)* **401**, 792 (1999).
- [16] T. J. Gawne, T. W. Kjaer, and B. J. Richmond, *J. Neurophysiol.* **76**, 1356 (1996).
- [17] M. Watanabe and K. Aihara, *Neural Networks* **10**, 1353 (1997).
- [18] R. C. DeCharms, D. T. Blake, and M. M. Merzenich, *Science* **280**, 1439 (1998).
- [19] M. P. Kilgard and M. M. Merzenich, *Nat. Neurosci.* **1**, 727 (1998).
- [20] V. Bringuier, Y. Fregnac, A. Baranyi, and D. Debanne, *J. Physiol. (Paris)* **500**, 751 (1997).
- [21] S. Molotchnikoff, S. Shumikhina, and L. E. Moisan, *Brain Res.* **731**, 91 (1996).
- [22] G. M. Ghose and R. D. Freeman, *J. Neurophysiol.* **68**, 1558 (1992).
- [23] C. Koch and G. Laurent, *Science* **284**, 96 (1999).
- [24] M. Steriade and F. Amzica, *Proc. Natl. Acad. Sci. U.S.A.* **93**, 2533 (1996).
- [25] M. Steriade, F. Amzica, and D. Contreras, *J. Neurosci.* **16**, 392 (1996).
- [26] M. Steriade, F. Amzica, and I. Timofeev, *J. Neurosci.* **16**, 2788 (1996).
- [27] M. Abeles, E. Vaddia, and H. Bergman, *Network* **1**, 13 (1990).
- [28] M. Abeles, H. Bergman, E. Margalit, and E. Vaddia, *J. Neurophysiol.* **70**, 1629 (1993).
- [29] M. Abeles, Y. Prut, H. Bergman, E. Vaddia, and A. M. H. J. Aertsen, *Brain Theory: Spatio-Temporal Aspects of Brain Function*, edited by A. Aertsen (Elsevier, Amsterdam 1993), pp. 149–181.
- [30] E. Vaddia, I. Haalman, M. Abeles, H. Bergman, Y. Prut, H. Slovin, and A. M. H. J. Aertsen, *Nature (London)* **373**, 515 (1998).
- [31] U. Leonards, W. Singer, and M. Fahle, *Vision Res.* **36**, 2689 (1996).
- [32] M. Usher and N. Donnelly, *Nature (London)* **394**, 179 (1998).
- [33] D. Alais, R. Blake, and S.-H. Lee, *Nat. Neurosci.* **1**, 160 (1998).
- [34] E. Bienenstock and C. von der Malsburg, *Europhys. Lett.* **5**, 121 (1987).
- [35] C. von der Malsburg and W. Schneider, *Biol. Cybern.* **54**, 29 (1986).
- [36] G. Wang, T. Tanaka, and M. Tanifuji, *Neurosci. Abstr.* **20**, 316 (1994).
- [37] E. D. Gershon, M. C. Wiener, P. E. Latham, and B. J. Richmond, *J. Neurophysiol.* **79**, 1135 (1998).
- [38] R. Lestienne and H. C. Tuckwell, *Neuroscience (N.Y.)* **82**, 315 (1998).
- [39] C. von der Malsburg and W. Schneider, *Biol. Cybern.* **54**, 29 (1986).
- [40] E. Bienenstock and C. von der Malsburg, *Europhys. Lett.* **5**, 121 (1987).
- [41] G. Laurent, K. MacLeod, M. Stopfer, and M. Wehr, *Learning and Memory* **5**, 124 (1998).
- [42] M. Abeles, *Corticonics: Neural Circuits of the Cerebral Cortex* (Cambridge University Press, New York, 1991).
- [43] M. Watanabe, K. Aihara, and S. Kondo, *Biol. Cybern.* **78**, 87 (1998).
- [44] Wolf Singer, *Curr. Opin. Neurobiol.* **9**, 189 (1999).
- [45] Z. F. Mainen and T. J. Sejnowski, *Science* **268**, 1503 (1995).